# Thermochromism in Copper(II) Complexes: Spectroscopic, Thermal, and Electrical Properties and Room-temperature Crystal Structure of Bis(2,2-dimethylpropane-1,3-diamine)copper(II) Dinitrate *

**Ledi Menabue and Gian Carlo Pellacani**
*Istituto di Chimica Generale e Inorganica, University of Modena, Via Campi 183, 41100 Modena, Italy*
**Luigi Pietro Battaglia and Anna Bonamartini Corradi**
*Istituto di Chimica Generale e Inorganica, Centro di Studio per la Strutturistica Diffrattometrica del C. N. R., University of Parma, Via D' Azeglio, 43100 Parma, Italy*
**Franco Sandrolini and Antonio Motori**
*Istituto Chimico, Facolta di Ingegneria, University of Bologna, Viale Risorgimento 2, 40136 Bologna, Italy*
**Russell J. Pylkki and Roger D. Willett**
*Chemistry Department, Washington State University, Pullman, Washington 99164, U.S.A.*

The compound bis(2,2-dimethylpropane-1,3-diamine)copper(II) dinitrate, $Cu(dmpd)_2(NO_3)_2$, undergoes a first-order thermochromic phase transition at 142 °C, changing colour from blue-violet to blue upon heating. The crystal structure determination of the low-temperature phase demonstrates that the copper ion has a distorted (4 + 2) octahedral geometry, with the two six-membered chelate rings forming the basal plane (Cu–N = 2.020, 2.029 Å), and oxygens from the two nitrate groups weakly co-ordinated in the fifth and sixth co-ordination sites (Cu–O = 2.566 Å). The i.r. data have been interpreted in terms of the presence of semi-co-ordinated nitrate ions in the low-temperature phase and of unco-ordinated nitrate ions in the high-temperature phase. The electronic spectra reveal a weakening of the ligand field in the high-temperature phase. The broadline n.m.r. indicates the onset of a dynamic disorder of the chelate rings upon heating through the phase transition. The weakening of the crystal field may be due to this dynamic disorder and/or the presence of a small tetrahedral distortion. Electrical conductivity measurements show interesting relaxation processes associated with the phase transition.

The phenomenon of thermochromism in inorganic materials is a subject of interest among co-ordination chemists. Two types of thermochromism have been identified in solids: a continuous thermochromism where the colour change is due to a gradual shift and/or broadening of the visible absorption bands upon thermal stress with an increased population of the ground-state vibrational levels, and a discontinuous thermochromism where the colour change is associated with a first-order structural phase transition. Studies of the latter type have recently been reviewed.[1] In many instances, the phase transition is triggered by the onset of a dynamic disorder of the organic constituents in the material, *e.g.*, of the ligand or counter ion. Recently a continuous thermochromism was reported[2] for a series of salts of the type $[Cu(dmpd)_2X_2]$ (X = Cl, Br, or $ClO_4$; dmpd = 2,2-dimethylpropane-1,3-diamine). In this paper we report the preparation and characterization of the corresponding nitrate salt, $Cu(dmpd)_2(NO_3)_2$, which displays discontinuous thermochromism.

## Experimental

The compound was prepared as described by Battaglia *et al.*[2] (Found: C, 30.60; H, 7.20; N, 21.40. Calc. for $C_{10}H_{28}CuN_6O_6$: C, 30.65; N, 7.20; N, 21.45%).

*Physical Measurements.*—The electronic spectra of the solid compounds were recorded as Nujol-mull transmission spectra with a Beckman DK 2A spectrophotometer in the 293—440 K temperature range. The temperature of the sample was determined with a thermocouple. Infrared spectra were recorded on a Perkin-Elmer 180 spectrophotometer as Nujol mulls on KBr discs in the range 250—4 000 $cm^{-1}$ and in Nujol mulls on polyethylene, as support, in the range 60—500 $cm^{-1}$. The i.r. spectra of the compound $Cu(dmpd)_2(NO_3)_2$ in the range 293—440 K were recorded between 500 and 1 300 $cm^{-1}$ as a powder on KBr discs using a Perkin-Elmer 457 spectrophotometer. The room-temperature e.s.r. spectra were recorded on a JEOL PE-3X spectrometer. Quartz sample tubes were used for polycrystalline samples. Spectra were calibrated with diphenylpicrylhydrazyl ($g = 2.0036$) as field marker. Differential scanning calorimetric (d.s.c.) analysis was performed with a Perkin-Elmer DSC-1 instrument. The broadline $^1H$ n.m.r. spectra were recorded on undeuteriated solid samples at 50 MHz using intrumentation previously described.[3] Powder *X*-ray diffraction patterns were run at 23, 138, and 145 °C.

*Electrical Measurements.*—Discs 28 mm in diameter and various thicknesses (up to 2 mm) suitable for the electrical measurements were prepared *in vacuo* under a pressure of 0.2 kN $mm^{-2}$. The samples were then sintered at 200 °C *in vacuo* in order to minimize intergranular effects and stabilize the material for the subsequent electrical measurements. Since preliminary measurements pointed out insulating properties of the materials at room temperature, a three-terminal technique was used for the electrical measurements. The voltmeter–ammeter method in d.c. (direct current) and bridge method in a.c. (alternating current) measurements were therefore used with the cell and instrumentation described elsewhere.[4-7] The samples were first coated with gold by vacuum evaporation and then measured from 190 °C to room temperature to avoid effects due to casual gas or vapour adsorption on the sample surface. D.c. measurements were made at a constant electrical field of 100 V $cm^{-1}$. Both charging and discharging currents were measured in order to observe

* *Supplementary data available* (No. SUP 23979, 12 pp.): thermal parameters, structure factors. See Instructions for Authors, *J. Chem. Soc., Dalton Trans.*, 1984, Issue 1, pp. xvii—xix.

*Non-S.I. unit employed:* G = $10^{-4}$ T.

**Table 1.** Final fractional co-ordinates ($\times 10^4$ for Cu, O, N, and C; $\times 10^3$ for H) with e.s.d.s in parentheses for $Cu(dmpd)_2(NO_3)_2$

| Atom | *X/a* | *Y/b* | *Z/c* |
|---|---|---|---|
| Cu | 0 | 0 | 0 |
| O(1) | −3 589(5) | 246(2) | −1 781(4) |
| O(2) | −5 066(5) | 763(2) | −4 045(5) |
| O(3) | −1 474(5) | 632(2) | −3 911(4) |
| N(1) | 1 741(6) | 874(2) | −671(5) |
| N(2) | −1 668(6) | 482(2) | 1 987(5) |
| N(3) | −3 378(5) | 551(2) | −3 262(4) |
| C(1) | 867(8) | 1 575(2) | −339(6) |
| C(2) | −47(6) | 1 683(2) | 1 548(5) |
| C(3) | −2 124(6) | 1 231(2) | 1 878(6) |
| C(4) | 1 745(7) | 1 553(2) | 2 974(6) |
| C(5) | −770(9) | 2 445(2) | 1 668(7) |
| H(1) | 300(8) | 79(2) | −4(6) |
| H(2) | 202(7) | 81(2) | −181(7) |
| H(3) | −60(7) | 163(2) | −129(6) |
| H(4) | 216(7) | 192(2) | −60(6) |
| H(5) | −333(7) | 126(2) | 97(6) |
| H(6) | −294(7) | 137(2) | 312(6) |
| H(7) | 312(7) | 186(2) | 279(6) |
| H(8) | 107(7) | 164(2) | 427(6) |
| H(9) | 225(7) | 100(2) | 300(6) |
| H(10) | −209(8) | 254(2) | 95(6) |
| H(11) | 54(7) | 284(2) | 137(6) |
| H(12) | −143(7) | 259(2) | 300(7) |
| H(13) | −89(8) | 36(2) | 288(7) |
| H(14) | −289(8) | 26(2) | 214(7) |

possible relaxation processes in the ultra-low frequency range,[7-10] usually due to structural effects in materials.

*Crystallographic Data Collection.—Crystal data.* $C_{10}H_{28}CuN_6O_6$, $M = 391.92$, monoclinic, $a = 5.951(1)$, $b = 19.333(3)$, $c = 7.457(2)$ Å, $\gamma = 91.00(1)°$, $U = 857.8$ Å$^3$, $D_m = 1.55$ g cm$^{-3}$ (by flotation), $Z = 2$, $D_c = 1.52$, $F(000) = 410$, $\mu(Cu\text{-}K_\alpha) = 19.8$ cm$^{-1}$, space group $P2_1/n$ (from systematic absences).*

Cell dimensions were initially obtained from rotation and Weissenberg photographs and later by least-squares refinement of the 2θ values of 15 reflections accurately measured on the diffractometer. The intensity data were collected using a crystal of dimensions 0.163 × 0.490 × 0.490 mm mounted with the [001] axis along the φ axis of an automated Siemens AED 'on line' single-crystal diffractometer using nickel-filtered Cu-$K_\alpha$ radiation (λ = 1 541 78 Å) and the ω–2θ scan technique in the range $6 \leqslant 2\theta \leqslant 140°$. In this way a total of 1 818 reflections were measured, 1 542 of these, having $I > 2\sigma(I)$, were used in the structural analysis. The structure amplitudes were obtained from the intensity data after correction for Lorentz and polarization factors and for absorption. The transmission factor ranged from 0.41 to 0.72. The absolute scale factor was determined first by Wilson's method, then as a variable parameter in the least-squares refinement.

*Structure determination and refinement.* The structure was solved by the heavy-atom technique fixing the copper atom at the origin of the cell. The successive Fourier synthesis gave all the non-hydrogen atoms. The refinements were carried out by full-matrix least squares by isotropic and anisotropic thermal parameters; the hydrogen atoms, located from a $\Delta F$ synthesis, were introduced in the final refinement with isotropic thermal parameters. The final $R$ index was 0.0348. The effects of the anomalous dispersion for Cu were included in all structure factor calculations. The function minimized in the least-squares refinement was $\Sigma|\Delta F|^2$, in which unit weights were adopted. 21 Reflections, probably affected by extinction or counting errors, were excluded from the final refinement. The atomic scattering factors were those of Cromer and Mann [11] for Cu, O, N, and C and those of Stewart *et al.*[12] for H. The final atomic co-ordinates are listed in Table 1. All calculations were performed on the Cyber 76 computer of the Centro di Calcolo Interuniversitario dell'Italia Nord Orientale, Bologna, using the SHELX system.[13]

* The conventional orientation can be obtained by applying the transformation matrix: 100/001/010.

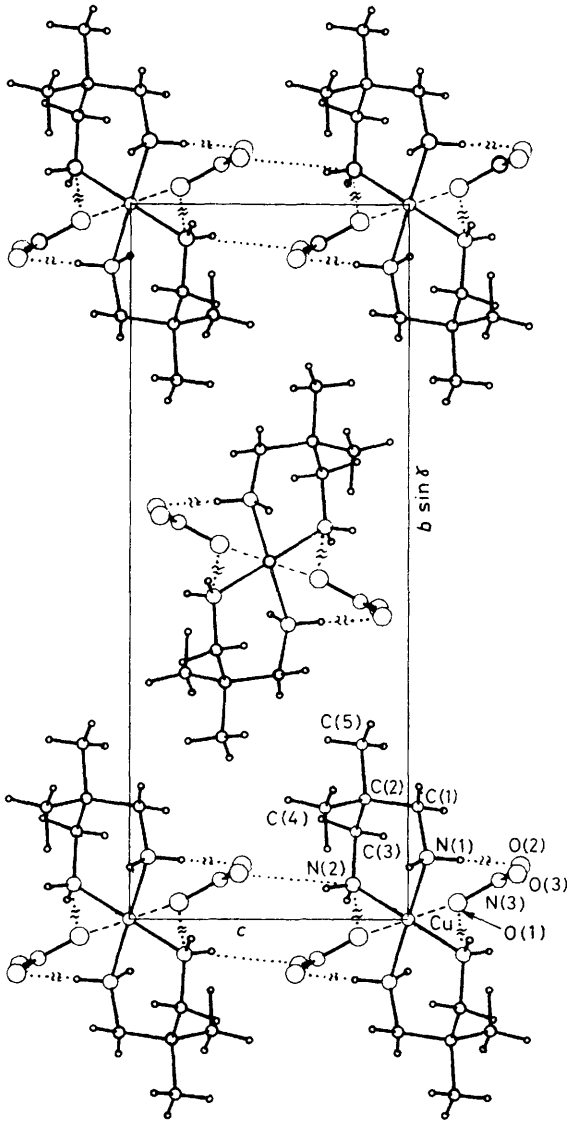


**Figure 1.** Projection of the structure of $Cu(dmpd)_2(NO_3)_2$ parallel to the [100] axis

## Results and Discussion

*Description of the Structure.*—The copper atom, located on the symmetry centre at the origin of the cell (Figure 1), co-ordinates four nitrogen atoms of two ligand molecules in a square-planar arrangement. Two oxygens from two centrosymmetrically related nitrate groups occupy further co-ordination sites forming an elongated tetragonal bipyramid. The angle of 8.9° formed between the line through the Cu–O(1)

**Table 2.** Bond distances (Å) and angles (°)

| | | | |
|---|---|---|---|
| Cu–O(1) | 2.566(3) | C(1)–H(3) | 1.17(4) |
| Cu–N(1) | 2.029(4) | C(1)–H(4) | 1.02(4) |
| Cu–N(2) | 2.020(3) | C(3)–H(5) | 0.99(4) |
| N(1)–C(1) | 1.480(5) | C(3)–H(6) | 1.13(4) |
| C(1)–C(2) | 1.524(7) | C(4)–H(7) | 1.02(4) |
| C(2)–C(4) | 1.529(5) | C(4)–H(8) | 1.06(4) |
| C(2)–C(5) | 1.544(5) | C(4)–H(9) | 1.09(3) |
| C(2)–C(3) | 1.521(5) | C(5)–H(10) | 0.97(4) |
| C(3)–N(2) | 1.480(5) | C(5)–H(11) | 1.10(4) |
| N(1)–H(1) | 0.90(4) | C(5)–H(12) | 1.10(5) |
| N(1)–H(2) | 0.87(5) | N(3)–O(1) | 1.257(4) |
| N(2)–H(13) | 0.85(5) | N(3)–O(2) | 1.237(4) |
| N(2)–H(14) | 0.84(5) | N(3)–O(3) | 1.239(4) |
| N(1)–Cu–N(2) | 92.56(2) | C(1)–C(2)–C(5) | 106.87(6) |
| N(1)–Cu–O(1) | 97.62(2) | C(4)–C(2)–C(5) | 108.85(5) |
| N(2)–Cu–O(1) | 82.93(2) | C(4)–C(2)–C(3) | 110.79(5) |
| Cu–N(1)–C(1) | 122.58(5) | C(3)–C(2)–C(5) | 107.54(5) |
| Cu–N(2)–C(3) | 120.73(4) | C(2)–C(3)–N(2) | 114.19(5) |
| N(1)–C(1)–C(2) | 114.30(6) | O(1)–N(3)–O(2) | 119.65(7) |
| C(1)–C(2)–C(3) | 111.04(6) | O(1)–N(3)–O(3) | 119.07(6) |
| C(1)–C(2)–C(4) | 111.57(7) | O(2)–N(3)–O(3) | 121.29(6) |

atoms and the normal to the Cu–N(1)–N(2) equatorial plane, and the angles on the copper indicate some further distortion of the co-ordination polyhedron. The Cu–N distances [2.029(4) and 2.020(3) Å, Table 2] are comparable with other values found in several copper(II)–amine complexes: bis(2,2-dimethylpropane-1,3-diamine)diperchloratocopper(II), 2.028(3) and 2.021(3) Å; [2] μ-carbonato-dichlorobis(*N*,*N*,*N*′,*N*′-tetramethylpropane-1,3-diamine)dicopper(II), 2.047(2)—2.043(2) Å; [14] and bis(*N*-methylpropane-1,3-diamine)nitratocopper(II) nitrate, 2.061(2)—2.009(2) Å.[15] The ligand molecules are arranged in a way quite similar to the previously cited perchlorate derivative, forming two six-membered chelate rings with the 'chair' conformation, the puckering parameters [16] being: $q_2 = 0.225$, $q_3 = -0.480$ Å, $\varphi_2 = 351.9°$, and $Q = 0.530$ Å ($q_2 = 0.219$, $q_3 = -0.502$ Å, $\varphi_2 = 349.6°$, and $Q = 0.53$ Å in the perchlorate derivative). The chair conformation is also found in other complexes containing six-membered chelate rings formed by aliphatic diamines.[17,18] The angles around the C(2) atom range from 106.87 to 111.57° (107.0—111.7° in the perchlorate complex). Bond distances and angles in the diamine (Table 2) agree very well with those found in these types of ligands.[2,14,15] The Cu–O(1) apical distance of 2.566(3) Å is typical of semi-co-ordination and is comparable with the value (2.602 Å) found in the perchlorate and in other nitrato-complexes, *e.g.*, in dinitrato(*N*,*N*,*N*′,*N*′-tetramethylethylenediamine)copper(II),[19] Cu–O = 2.612(6) Å.

The nitrate groups, which show the regular trigonal-planar geometry, are involved in the hydrogen-bond system and intramolecular contacts [Table 3(*a*) and (*b*), respectively], which are responsible for the packing in the crystal. Some systematic distortion exists, due to the interaction of the $NO_3^-$ group with the $Cu^{2+}$ ion.

*D.S.C., Thermogravimetric (T.g.), E.S.R., and Spectroscopic Results.*—The d.s.c. analysis shows a sharp endothermic peak in the temperature range 142—152 °C corresponding to a thermochromic phase transition. The transition is reversible. T.g. analysis further shows no weight change in this temperature range. The $\Delta H$ value of *ca.* 10.6 kJ mol$^{-1}$ (averaged value) is in good agreement with those previously found for some fluoroborate and perchlorate copper(II) complexes of substituted ethylenediamines, but lower than that reported for the analogous nitrate.[20]

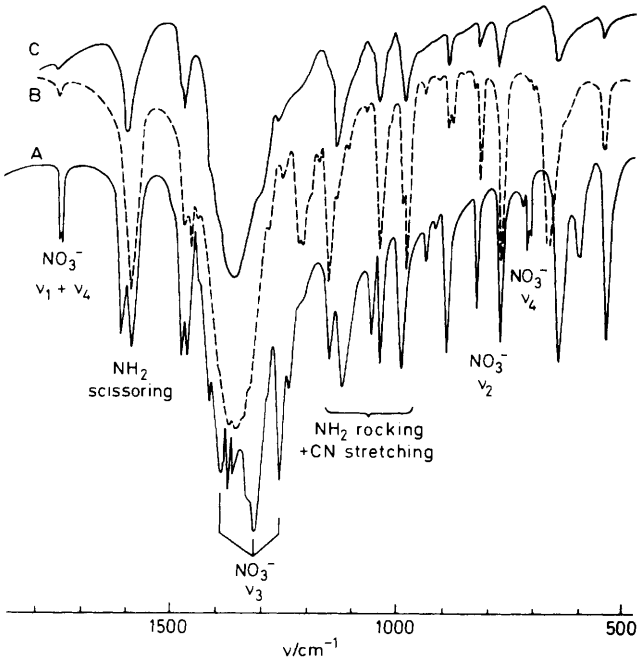


**Figure 2.** Comparison of the i.r. spectra of $Cu(dmpd)_2(NO_3)_2$ [20—120 °C (A) and 160 °C (C)] and of $Zn(dmpd)_2(NO_3)_2$ [20 °C (B)]. All spectra were run as powder on KBr pellets as support

The role of the anion in determining the phase transition is well established by the study of the i.r. spectrum of the compound at variable temperatures. In fact, in the 20—135 °C temperature range the position and number of fundamental modes of nitrate groups are characteristic of monodentate-bound nitrate groups. Furthermore the splittings of the bands assignable to $NH_2$ vibrations [21] are consistent with the presence of substantial interactions between the nitrate and the amino-groups. This agrees with the structural data. To support our assignments in Figure 2 we have also reported the i.r. spectrum of the analogous $Zn^{II}$ and $Pd^{II}$ complexes.[22] For the latter two, unco-ordinated nitrate ions may be certainly suggested.

The i.r. spectrum of the copper(II) complex shows a dramatic change at the same temperature as the phase transition determined by d.s.c. measurements. At temperatures greater than 155 °C the spectrum is very similar to that of the zinc(II) salt, indicating a decrease of the interactions between the nitrate groups and the copper(II) ion (Figure 2).

The corresponding Pd compound has been prepared, and its i.r. spectrum has been recorded. The spectrum of the low-temperature phase of the Cu complex most closely resembles that of the Pd compound (trace A, Figure 2), while the high-temperature phase (trace C) has many features common with the tetrahedral Zn complex (trace B). This lends supporting evidence for the supposition that a tetrahedral distortion occurs in the high-temperature phase of the copper compound.

The powder *X*-ray diffraction pattern has been recorded immediately below and above the phase transition temperature. The patterns of the two phases are significantly different. However, many of the diffraction lines of the low-temperature phases are reproduced in the high-temperature pattern with a small shift to lower Bragg angles (larger *d* spacings). Thus, a major change in unit-cell shape does not appear to take place. Nevertheless, major intensity changes occur, for a few diffraction lines, indicating a substantial change in internal structure. The above data, although inconclusive, are not in-

**Table 3.** Hydrogen bond system and some contacts less than 3.50 Å

(*a*) Hydrogen bonds

| | | | | | |
|---|---|---|---|---|---|
| N(1) · · · O(2$^{II}$) | 3.162(5) | | | | |
| N(1)–H(2) | 0.87(5) | H(2) · · · O(2$^{II}$) | 2.40(5) | N(1)–H(2) · · · O(2$^{II}$) | 145(5) |
| N(2) · · · O(3$^{III}$) | 3.074(4) | | | | |
| N(2)–H(13) | 0.85(5) | H(13) · · · O(3$^{III}$) | 2.46(5) | N(2)–H(13) · · · O(3$^{III}$) | 128(6) |
| N(2) · · · O(1$^{IV}$) | 3.136(5) | | | | |
| N(2)–H(14) | 0.84(4) | H(14) · · · O(1$^{IV}$) | 2.31(4) | N(2)–H(14) · · · O(1$^{IV}$) | 164(4) |

(*b*) Contacts

| | | | |
|---|---|---|---|
| N(1) · · · O(1) | 3.476(4) | O(3) · · · C(4$^{VII}$) | 3.480(5) |
| N(1) · · · O(3) | 3.112(5) | O(3) · · · O(3$^{VIII}$) | 3.440(5) |
| N(2) · · · O(1) | 3.064(5) | N(2) · · · O(3$^{I}$) | 3.214(5) |
| O(1) · · · C(3) | 3.431(5) | N(1) · · · O(1$^{I}$) | 3.053(5) |
| O(3) · · · C(1) | 3.503(6) | O(1) · · · O(1$^{IV}$) | 3.274(4) |
| O(2) · · · C(4$^{V}$) | 3.313(5) | O(2) · · · N(2$^{IV}$) | 3.429(5) |
| O(2) · · · N(3$^{VI}$) | 3.355(5) | O(1) · · · N(2$^{I}$) | 3.456(5) |
| O(2) · · · O(2$^{VI}$) | 3.278(5) | O(2) · · · C(4$^{VI}$) | 3.313(5) |
| O(3) · · · C(3$^{VII}$) | 3.371(5) | O(3) · · · N(2$^{VII}$) | 3.074(5) |

Symmetry operators: I = $\bar{x}, \bar{y}, \bar{z}$; II = $1 + x, y, z$; III $x, y, 1 + z$; IV = $\bar{x} - 1, \bar{y}, \bar{z}$; V = $x - 1, y, z - 1$; VI = $\bar{x} - 1, \bar{y}, \bar{z} - 1$; VII = $x, y, z - 1$; VIII = $\bar{x}, \bar{y}, \bar{z} - 1$.

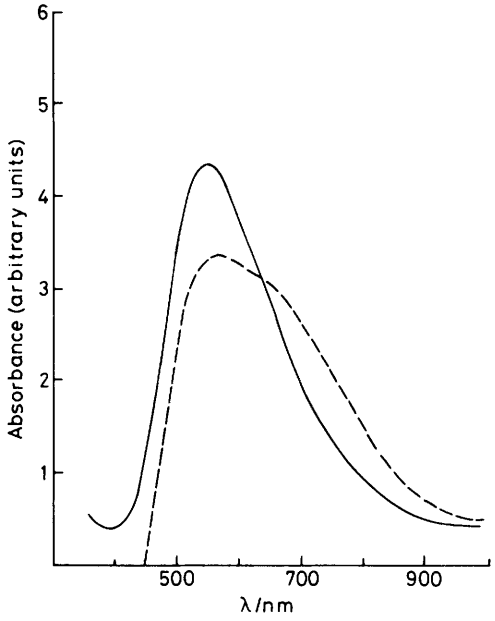


**Figure 3.** Electronic spectra of $Cu(dmpd)_2(NO_3)_2$ below [20—120 °C (——)] and above [160 °C (– – – –)] the phase transition

consistent with a tetrahedral distortion and a weakening of the Cu–$NO_3$ interactions in the high-temperature phase.

The room-temperature e.s.r. parameters ($g_{\parallel} = 2.176$ and $g_{\perp} = 2.055$), typical of tetragonal bipyramidal complexes with a $d_{x^2-y^2}$ ground state and a $CuN_4O_2$ chromophore [2] are consistent with the structural results. The only change observed in the e.s.r. spectrum of the high-temperature phase was a broadening of the linewidths, which washed out the $g_{\parallel}$ region. An increase in tetragonality (*e.g.*, weakening of the semi-co-ordination) should lead to a decrease in the $g$ values, while a tetrahedral distortion has the opposite effect. Thus, the lack of shift in the position of $g_{\perp}$ is consistent with the existence of both of these two competing factors.

These results, combined with the lowering and splitting of the *d–d* bands in the high-temperature phase (Figure 3), imply a tetrahedrally distorted four-co-ordinated geometry at high temperatures. Similar results were previously suggested for the analogous copper(II) perchlorate complex, which displayed a continuous thermochromism.[2]

*Electrical Results.*—The electrical conductivity derived from the charging currents at 1 and 10 min after the application of the voltage exhibits two distinct conduction regions with different apparent activation energy, with the higher activation energy present in the high-temperature range (Figure 4).

The behaviour exhibited in the isochronal discharging currents as a function of temperature is shown in Figure 5. A peak can be seen, at 140 °C, which must be related to a relaxation process occurring below $10^{-2}$ Hz at such a temperature. The same transition is observed in the isothermal discharging currents as functions of time (not shown for the sake of brevity).

Dielectric measurements in the range $2 \times 10^{-2}$—$6 \times 10^{5}$ Hz do not show remarkable effects in the temperature range investigated. The relative dielectric constant and loss factor regularly decrease with frequency up to a constant value of 3.93 and 0.005, respectively, at room temperature. At higher temperatures the behaviour does not change although the curves are shifted to higher frequency.

The close resemblance of the behaviour of electrical conductivity with that typically shown from semiconducting compounds suggests that the conduction mechanism is basically electronic. This is confirmed by the low value of dielectric constant (except for the ultra-low frequency range) and the absence of any ionic effect in the loss factor as a function of frequency. The peak observed in the isochronal discharging currents curves at 140 °C (Figure 5) discloses, on the other hand, a typical dielectric relaxation process well below the low frequencies investigated with the instrumentation used.[6,8–10] It may be due, therefore, to neither electronic nor atomic polarization processes, but to processes involving larger structural units or some polarization of the Maxwell–Wagner–Sillars type. It can be therefore related to the above discussed structural changes occurring near 140 °C, which perturb the transport of the charge carriers. Moreover, it may be inferred that the study of the electrical properties is of substantial aid in evaluating structural transitions in these materials. Further investigations would be needed to determine the type of majority charge carrier and the other semiconducting prop-

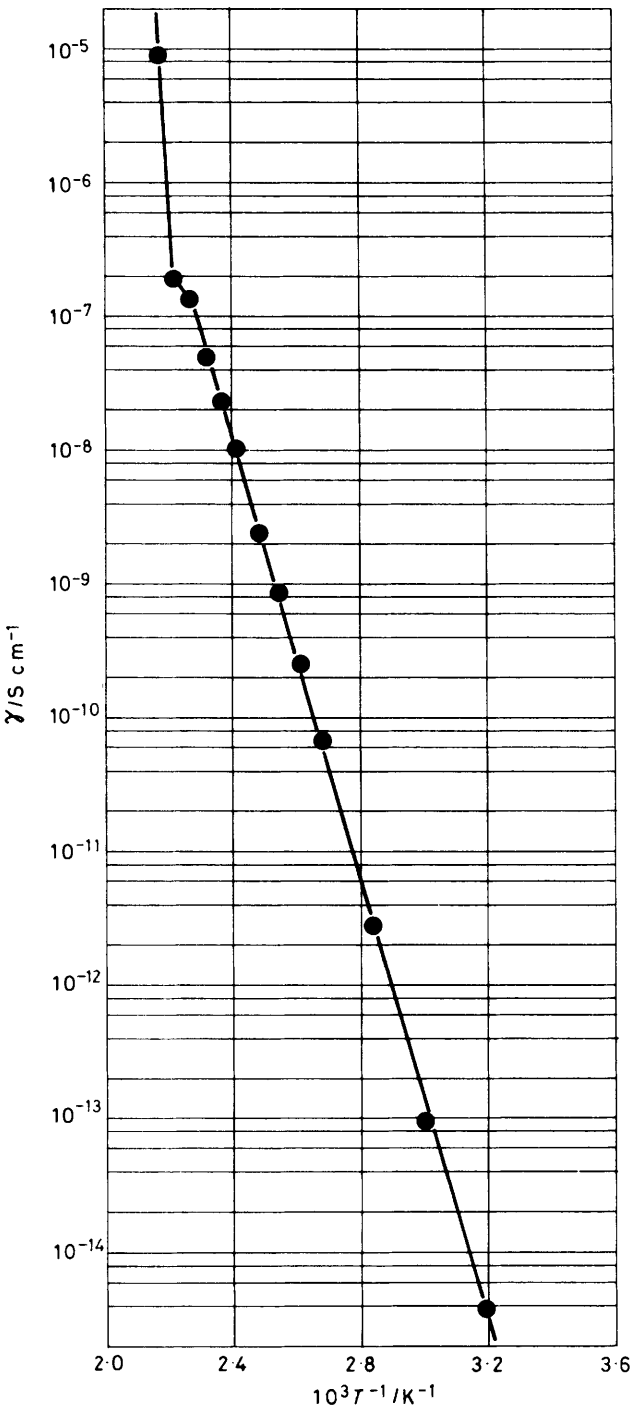


**Figure 4.** Electrical conductivity (log scale) of $Cu(dmpd)_2(NO_3)_2$ after 10 min of voltage application *vs.* $10^3T^{-1}$

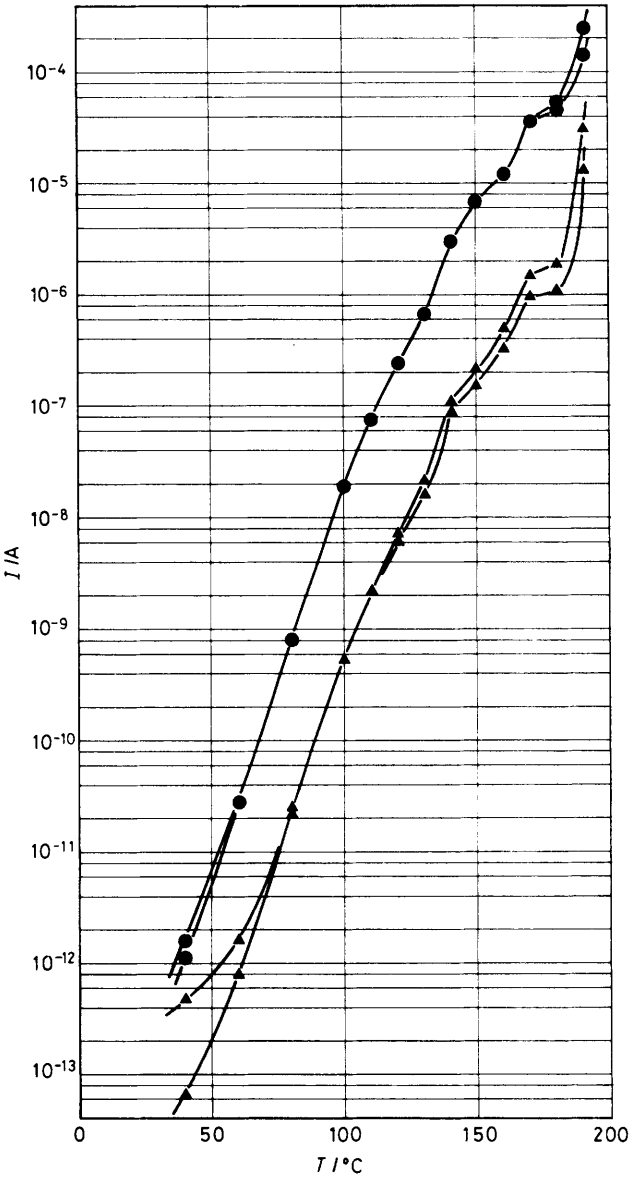


**Figure 5.** Charging (●) and discharging (▲) [upper curve: 1 min after voltage application; lower curve: 10 min after voltage application] currents *vs.* temperature for $Cu(dmpd)_2(NO_3)_2$

erties of the material, as well as the exact nature of the dielectric processes occurring at the transition temperature ($T_c$).

*Broadline N.M.R. Results.*—A $^1H$ broadline n.m.r. study of the behaviour of the compound in the vicinity of the structural phase transition was made. The second moment ($M_2$) of the resonance line was obtained by integration of the observed spectrum as given in equation (1), where $H_o$ is the field at the centre of the resonance signal and $I(H-H_o)$ is the intensity at a given field, $H$. The results are shown in Figure 6. As can

$$M_2 = \frac{\int I(H-H_o)(H-H_o)^2\,dH}{\int I(H-H_o)\,dH} \qquad (1)$$

be seen, a sharp drop in the second moment from 22 $G^2$ to 15 $G^2$ occurs at 142 °C. This transition temperature agrees well with the d.s.c. results. The pronounced decrease in second moment clearly indicates the onset of some dynamic disorder. We will seek to make a deduction concerning the type of disorder from the magnitude of the reduction factor, $R$ [$R = M_2(T > T_c)/M_2(T < T_c) \sim 0.7$].

Theoretically, we can calculate the reduction factors for powder samples for several possible types of motion using equations (2) and (3),[23] where $r_{ij}$ is the vector between the $i$th and $j$th proton, $\theta_{ij}$ is the angle between the magnetic field and $r_{ij}$, and the integrals are over all possible orientations of the $r_{ij}$ vector. The thermal average $[\langle(3\cos^2\theta_{ij}-1)^2\rangle_{av.}]$ in $M_2$(dynamic) is obtained by taking a sum over the $N$ configurations assumed by the molecule. The reduction

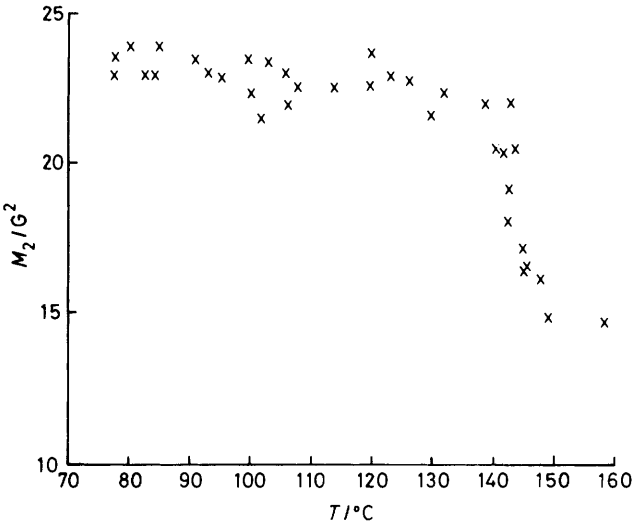


**Figure 6.** Plot of $^1H$ n.m.r. second moment *versus* temperature for $Cu(dmpd)_2(NO_3)_2$

$$M_2(\text{static}) \propto \sum_{i>j} \int_0^{2\pi}\int_0^{\pi} \frac{(3\cos^2\theta_{ij}-1)^2}{r_{ij}^6}\, d\theta_{ij}d\varphi_{ij} \quad (2)$$

$$M_2(\text{dynamic}) \propto \sum_{ij} \int_0^{2\pi}\int_0^{\pi} \frac{(\langle 3\cos^2\theta_{ij}-1\rangle_{av.}-1)^2}{r_{ij}^6}\, d\theta_{ij}d\varphi_{ij} \quad (3)$$

$$\langle(3\cos^2\theta_{ij}-1)^2\rangle_{av.} = \frac{1}{N}\sum_{l=1}^{N}\frac{(3\cos^2\theta_{ij}-1)^2}{r_{ij}^6} \quad (4)$$

factor is then given by equation (5). For simplicity, only

$$R = \frac{M_2(\text{dynamic})}{M_2(\text{static})} \quad (5)$$

contributions from proton–proton interactions on a single carbon atom are included.

The *X*-ray diffraction results show that the stable configuration for each six-membered metal–chelate ring is the chair configuration. One possible type of motion to consider is that the ring interchanges between two equivalent chair configurations. This seems unlikely because the interchange cannot occur in one simple motion and because it causes large displacement of C(3), C(4), and C(5). The latter would imply major rearrangement of other portions of the crystal structure during the interchange, which does not seem plausible. The calculation of the reduction factors confirms this, with *R*-(calc.) = 0.5 compared to the experimental value of 0.7. A second type of motion is the interchange between the chair configuration and a boat configuration by displacement of C(2). However, this places one of the methyl groups within ~2 Å of the position of the nitrate ion. The most probable rearrangement involves a twist about the normal to one of the C–N bonds, changing the chair configuration into a boat configuration. This motion involves very little displacement of C(2) or the methyl groups. The summation in equation (4) is now over three configurations; two equivalent boat forms and the original chair form. The reduction factor estimated for this motion is in satisfactory agreement with the experimental result. Thus, we conclude that the higher temperature phase involves a dynamic equilibrium between these three configurations of the metal–chelate rings.

## Conclusions

The thermochromism of bis(2,2-dimethylpropane-1,3-diamine)copper(II) dinitrate must be ascribed to the weakening of the in-plane ligand-field strength, as the temperature is raised, due to a dynamic disorder of the chelate rings of the ligand and the presence of a small tetrahedral distortion. As a consequence, the nitrate anions are not as strongly coordinated in the high-temperature form. This is in contradistinction to the behaviour of bis(*N*,*N*-diethylethylenediamine)copper(II) dinitrate.

The investigated salt exhibits interesting semiconducting properties and the electrical measurements seem to be very useful in investigating the thermochromic behaviour of these compounds: dielectric relaxation processes related to the structural changes indeed do occur at the phase transition.

## Acknowledgements

We thank the University of Parma for financial support.

## References

1 D. R. Bloomquist and R. D. Willett, *Coord. Chem. Rev.*, 1982, **47**, 125.
2 L. P. Battaglia, A. Bonamartini Corradi, G. Marotrigiano, L. Menabue, and G. C. Pellacani, *J. Chem. Soc., Dalton Trans.*, 1981, 8.
3 D. R. Bloomquist, S. A. Roberts, R. D. Willett, and H. W. Dodgen, *J. Am. Chem. Soc.*, 1981, **123**, 2603.
4 F. Sandrolini and P. Manaresi, *J. Polym. Sci., Polym. Chem. Ed.*, 1976, **14**, 939.
5 F. Sandrolini and P. Cremonini, *Mater. Plast. Elastomeri.*, 1979, 405.
6 F. Sandrolini and P. Manaresi, 26th Int. Symp. Macromol. IUPAC, Mainz, 1979, eds. I. Luderwald and R. Weis, vol. 3, p. 1463.
7 F. Sandrolini, *J. Phys. E*, 1980, **13**, 152.
8 B. V. Hamon, *Proc. IEEE*, 1952, **99**, 151.
9 M. E. Baird, *Rev. Mod. Phys.*, 1968, **40**, 219.
10 V. D. Shthraus, *Mekh. Polim.*, 1976, **12**, 507.
11 D. J. Cromer and J. B. Mann, *Acta Crystallogr., Sect. A*, 1968, **24**, 321.
12 R. F. Stewart, E. R. Davidson, and W. T. Simpson, *J. Chem. Phys.*, 1965, **42**, 3175.
13 G. Sheldrick, SHELX 76 system of computer programs, University of Cambridge, 1976.
14 M. Rowen Churchill, G. Davis, M. A. El-Sayed, M. F. El-Shazly, J. P. Hutchinson, M. W. Rupich, and K. O. Watkins, *Inorg. Chem.*, 1979, **18**, 2296.
15 U. Turpeinen, R. Hämäläinen, and M. Ahlgrén, *Cryst. Struct. Commun.*, 1978, **7**, 241.
16 D. Cremer and J. A. Pople, *J. Am. Chem. Soc.*, 1975, **97**, 1354.
17 G. D. Andreetti, L. Cavalca, and P. Sgarabotto, *Gazz. Chim. Ital.*, 1971, **101**, 483, 494.
18 G. C. van Kralingen, J. Reedijk, and A. L. Spek, *Inorg. Chem.*, 1980, **19**, 1481 and refs. therein.
19 M. Nasakkala and A. Pajunen, *Cryst. Struct. Commun.*, 1980, **9**, 897.
20 L. Fabbrizzi, M. Micheloni, and P. Paoletti, *Inorg. Chem.*, 1974, **13**, 3019.
21 T. G. Appleton and J. R. Hall, *Inorg. Chem.*, 1970, **9**, 1800.
22 G. C. Pellacani, unpublished work.
23 J. C. Crowley, H. W. Dodgen, and R. D. Willett, *J. Phys. Chem.*, 1982, **86**, 4046.

*Received* 1*st February* 1983; *Paper* 3/149